ORIGINAL ARTICLE

Changes in cell wall components and hygroscopic properties of *Pinus radiata* caused by heat treatment

Alberto García-Iruela[1] · Luis García Esteban[1] · Francisco García Fernández[1] · Paloma de Palacios[1] · Alejandro B. Rodriguez-Navarro[2] · Raquel Martín-Sampedro[3] · María Eugenia Eugenio[4]

Abstract

After thermal modification at 210 °C using the Thermowood method, changes in *Pinus radiata D.* Don wood cell wall components and hygroscopicity were studied for subsequent comparison with recently felled wood of the same species in samples from the same region of provenance (Basque Country, Spain). To this end, samples were characterised by sorption isotherms at 15, 35 and 50 °C fitted to the Guggenheim–Anderson–de Boer (GAB) model, the chemical composition was obtained by high performance liquid chromatography (HPLC) and infrared spectroscopy (FTIR), and crystallinity and structural organisation of cellulose (crystal orientation) were determined using powder and 2D X-ray diffraction (XRD). Heat treatment caused the following changes in the wood: a decrease in the equilibrium moisture content (EMC); a smaller hysteresis area and therefore more hygroscopically stable wood; a decrease in the hemicellulose content; an increase in the relative percentage of cellulose, lignin and extractives; and a higher degree of crystallinity and crystal orientation of the cellulose. The reorganisation of cellulose could be explained by epitaxial growth of cellulose starting from the highly oriented crystalline regions during the recrystallisation process. All these chemical and structural changes induced by heating could explain the reduction in hygroscopic properties of wood, as well as its stability.

1 Introduction

Many studies have demonstrated that heat treatment decreases wood equilibrium moisture content (Hill et al. 2012; Olek et al. 2012; Rautkari et al. 2013; Kymäläinen et al. 2015, 2018; Sun et al. 2017; Hosseinpourpia et al. 2017, 2018; Li et al. 2017; Wang et al. 2018; Tarmian and Mastouri 2019), improves wood dimensional stability (Militz 2002; Čermák et al. 2015) and decay resistance (Kim et al. 1998; Kamdem et al. 2002; Hakkou et al. 2006; Boonstra et al. 2007). This allows thermally modified wood to be used in less favourable conditions and improves its competitiveness with more costly tropical timbers. The main disadvantage of this process is the decrease in wood bending properties (Kim et al. 1998; Hill 2006; Rautkari et al. 2014). However, little is known about the response of cell

✉ Alberto García-Iruela
  agiruela17@gmail.com

  Luis García Esteban
  luis.garcia@upm.es

  Francisco García Fernández
  francisco.garcia@upm.es

  Paloma de Palacios
  paloma.depalacios@upm.es

  Alejandro B. Rodriguez-Navarro
  anava@ugr.es

  Raquel Martín-Sampedro
  r.martin.sampedro@csic.es

  María Eugenia Eugenio
  mariaeugenia@inia.es

[1] Departamento de Sistemas Y Recursos Naturales. Cátedra de Tecnología de La Madera. Escuela Técnica Superior de Ingenieros de Montes, Forestal Y del Medio Natural, Universidad Politécnica de Madrid. Ciudad Universitaria, 28040 Madrid, Spain

[2] Departamento de Mineralogía Y Petrología, Universidad de Granada, Av. Fuentenueva, 18002 Granada, Spain

[3] Departamento de Nuevas Arquitecturas en Química de Materiales, Instituto de Ciencia de Materiales de Madrid (ICMM-CSIC), Sor Juana Inés de la Cruz 3, Cantoblanco, 28049 Madrid, Spain

[4] Instituto Nacional de Investigación Y Tecnología Agraria Y Alimentaria, INIA, Carretera de La Coruña, km 7.5, 28040 Madrid, Spain

wall components (especially their reorganisation) to this and other treatments.

Some authors have attempted to explain hygroscopic behaviour in thermally modified wood based on the changes in wood cellulose crystallinity using FTIR (Yildiz and Gümüskaya 2007; Rautkari et al. 2013; Wang et al. 2018; Tarmian and Mastouri 2019) or XRD (Segal et al. 1959). However, the crystallinity index (CrI) value for a given sample can vary significantly depending on the measuring technique chosen and the calculation method used (Evans et al. 1995; Thygesen et al. 2005; He et al. 2008).

Methods based on XRD typically produce CrI values that vary in the following order: XRD height method > XRD amorphous subtraction > XRD peak deconvolution > Nuclear Magnetic Resonance (NMR) (Park et al. 2010).

Because different crystallinity determination techniques measure different parameters, complete agreement among methods or a direct comparison of results between studies is not always possible. The Segal equation (Segal et al. 1959), the most widely used method to assess crystallinity in cellulose, has been criticised, in particular because the area under the peaks is more important than the height of the peaks. Although this is the most commonly used method in the literature, numerous studies advise against it (Thygesen et al. 2005; Park et al. 2010; French and Santiago Cintrón 2013). The amorphous subtraction method, like the Segal peak height method, depends on the assumption that the diffraction intensity at the valley between the (110) and (200) peaks is due to amorphous material and, therefore, has inherent defects. The XRD deconvolution method is more solidly based. In this method, software is needed to separate amorphous and crystalline contributions to the diffraction pattern using a curve-fitting process. Certain assumptions must be made for the curve fitting, for example the shape and number of peaks (Park et al. 2009). However, this method is still imprecise, because it is usually performed with curve-fitting software that does not account for the specific problems of diffraction data, such as the preferred orientation and crystal size anisotropy typical of cellulose materials. Moreover, normally only a few strong peaks are included, together with a wide curve defining the amorphous contribution to the overall intensity. Thus, none of the conventional methods for studying crystallinity by diffraction are satisfactory and more sophisticated methods that consider the influence of preferred orientation (texture) and crystal size anisotropy are needed (Bonarski and Olek 2011; Olek and Bonarski 2014; García-Iruela et al. 2019).

In this study, the Rietveld method of refining powder diffraction data (Rietveld 1969; Young 1993) combined with 2D X-ray diffraction was used. The Rietveld method appears to be the most reliable approach for studying cellulose crystallinity and has been applied by several researchers (e.g. Thygesen et al. 2005; Kim et al. 2018; Ling et al. 2019). In

this method, the experimental diffraction pattern is fitted to theoretical diffraction patterns calculated from the structure of each crystalline phase present in the sample (Nishiyama et al. 2002). The 2D X-ray diffraction method was also applied to measure dispersion in the cellulose crystal orientation, as well as the crystallinity and proportion of preferentially and randomly oriented cellulose fractions. The crystallinity was determined from the peak broadening of (200) and (004) cellulose Iβ reflections to account for crystallite anisotropy. This 2D X-ray diffraction method provides new and additional information about the structural reorganisation and recrystallisation of cellulose during heating.

The objective of this study was to compare the hygroscopic response of recently felled (untreated) and *Pinus radiata* D. Don wood thermally modified at 210 °C by the Thermowood method, and examine how changes in the cell wall components, cellulose structural reorganisation and recrystallisation during heating can explain the effect of heat change on hygroscopicity.

2 Material and methods

2.1 Provenance of samples

Pinus radiata D. Don wood was obtained from plantations in the Lombrade forest in the municipality of Zeanuri (Biscay, Spain). Five trees, 47–57 cm in diameter, were felled at 1.30 m height. From the first log of about 1000 mm in length, 10 pieces were cut with 25 mm thickness, 40 mm width and 500 mm length between rings 25 and 30, five to obtain the samples of untreated wood and the other five for thermally modified wood. To determine EMC, chemical composition, FTIR and XRD-diffraction, strips were obtained from each untreated and thermally modified board by manual planing (approx. 15 mm long, 10 mm wide and 1 mm thick). The number of replicates was five for EMC and 10 for the other properties.

The heat treatment was performed industrially at 210 °C using the Thermowood method, in which wood is heated to 185–215 °C in a dryer while steam is injected, maintaining a constant temperature for 2–3 h. The temperature is then lowered by water spraying until the wood reaches a moisture content of 4–7% (for more details of this process see ThermoWood® Handbook 2003).

2.2 Sorption isotherms

The 15°, 35 °C and 50 °C sorption isotherms were plotted using the COST Action E8 saturated salt method (Jowitt and Wagstaffe 1989). The water activities for the salts at 15°, 35° and 50° were taken from Baxter and Cooper (1924), Acheson (1965), Greenspan (1977), Huang (1985) and Clarke

and Glew ([1985]). The desorption isotherm of the recently felled wood was plotted before its moisture content dropped below the saturation point, to avoid possible hysteresis peaks that could have resulted in misinterpretation of the sorption loops (Fredriksson and Thybring [2018]). The sorption cycle of the modified wood also began in desorption at the start of treatment. The heat-treated wood was resaturated by vacuum with deionised water, following the method used by Fredriksson and Thybring ([2018]). Equilibrium was considered to have been reached in each salt when the weight difference was no more than 0.1% when samples were weighed in a 24 h interval.

The Guggenheim–Anderson–de Boer (GAB) model was used. Because of the good fit of the sigmoid to the EMC obtained in lignocellulosic materials, this model is widely applied (Avramidis [1997]) (Eq. [1]).

$$X = \frac{K \cdot C_g \cdot a_w}{(1 - K \cdot a_w)(1 - K \cdot a_w + C_g \cdot K \cdot a_w)} \cdot X_m \qquad (1)$$

where X EMC (%); X_m monolayer saturation moisture content (%); C_g Guggenheim constant (dimensionless); K constant (dimensionless); a_w water activity on a scale of zero to one (dimensionless).

The fit was considered valid when the correlation coefficient R was higher than 0.999 and the root mean square error (RMSE) was lower than 4% (Esteban et al. [2008a], [b], [2009]).

2.3 Chemical composition and number of accessible –OH groups

The untreated wood and thermally modified wood were chemically analysed to determine possible changes in the cell wall components.

The extractives were obtained with ethanol, following the standard procedure of Sluiter et al. ([2005]), and the lignin and sugar percentages were determined using double hydrolysis (Sluiter et al. [2012]). Sugar content was quantified by high performance liquid chromatography in an Agilent Technologies 1260 HPLC that included an Agilent Hi-Plex Pb column and an RI-detector system. Separation was performed at 70 °C with a flow of 0.6 ml min^{-1}, with water as the mobile phase. The percentage of cellulose and hemicellulose (hexoses and pentoses) was determined from the amount of sugars (Easty and Malcolm [1982]; Jones et al. [2006]).

Infrared spectroscopy (FTIR) was used as a qualitative tool to identify the functional groups. Sawdust samples of the two types of wood (untreated and thermally modified) were prepared and all the samples were oven dried for 24 h at 103 ± 2 °C and then cooled in a desiccator with silica gel at room temperature. A disc with 3 mg dry sawdust was pressed against the ATR diamond crystal window, recording spectra after 64 scans at 4 cm^{-1} resolution using a Spectra-Tech Performer spectrophotometer (Thermo Fisher Scientific, Waltham, MA, USA). The powdered sample was placed so that it completely covered the ATR diamond crystal window. Before each sample was taken, the background was measured under the same conditions as with no sample in the ATR. To determine the heights of the IR peaks corresponding to the functional groups, two points were used for the baseline background correction.

Although other methods can be used to determine the theoretical –OH group content, such as in Supplementary material by Thybring et al. ([2017]), the accessible –OH content, in moles per gram of dry wood, was calculated using Rowell's equation, adjusting the cellulose with the crystallinity index, given that the –OH of the crystalline portion are inaccessible (Rowell [1980]; Hill and Jones [1996], [1999]; Hill [2006]; Hill et al. [2010]; Rautkari et al. [2013]) (Eq. [2]).

$$OHgroup_t = \frac{3A}{162} + \frac{3B}{162} + \frac{2C}{132} + \frac{D}{180} \qquad (2)$$

where $OHgroup_t$ Number of theoretical –OH groups; A cellulose content (%); B hexosan hemicellulose content (%); C pentose hemicellulose content (%); D lignin content (%).

2.4 Cellulose crystallinity and crystal orientation by X-ray diffraction

2.4.1 Powder X-ray diffraction

The crystalline phase content and crystallinity of the wood chip samples were analysed by X-ray diffraction using an Xpert Pro X-ray powder diffractometer (Panalytical, The Netherlands) in reflection mode and copper radiation to determine theta-2theta scans (from 10° to 45° with 0.03° step size and 235 s integration time per step). Rietveld refinement analyses of XRD profiles were conducted using Topas 5.0 software (Bruker, Germany) to determine cellulose polymorphic phases, unit cell parameters and crystallite size. Two cellulose phases were included in the model: crystalline cellulose Iβ and amorphous cellulose. Amorphous cellulose was simulated as cellulose II with 12 Å crystallite size, according to the methodology described by French and Kim ([2018]). The parameters refined using Topas software were crystallite size and cellulose Iβ unit cell parameters, as well as the weight fraction of each cellulose phase.

2.4.2 Two-dimensional (2D) X-ray diffraction

Small pieces of wood (1×1 cm) were analysed with a single crystal diffractometer equipped with a PHOTON area detector (D8 Venture, Bruker, Germany) and Cu radiation (120 s). Samples were measured in transmission mode with their fibres oriented perpendicular or parallel to the X-ray beam. Wood crystallinity was determined by measuring the

full width at half maximum (FWHM) of the main cellulose peaks (e.g., 004, 200) displayed in 2Theta scan, calculated by radially integrating intensities from 2D X-ray diffraction patterns. At sharper peaks and smaller FWHM, crystallinity was greater. The Scherrer equation was used to estimate cellulose crystallite size. A quantitative estimation of the degree of alignment of the c-axis of cellulose crystals in the wood samples was determined from the angular width of bands displayed in the intensity profile along the Debye–Scherrer ring (Gamma scan) associated with the 200 reflection of cellulose. The wider the band, the greater the scattering was in the orientation of the c-axis of cellulose crystals. The crystallinity and proportion of preferentially and randomly oriented cellulose were determined from the 2D pattern, following the methodology described elsewhere (García-Iruela et al. 2019). Two-dimensional XRD patterns were analysed using XRD2DScan software version 7.0 (PANalytical, The Netherlands).

2.5 Statistical analysis

The statistical analysis was performed using Statistics Toolbox® ver. 6.1 MATLAB® ver. 7.5.0 Release 2007b.

The isotherms and the confidence intervals of the parameters were obtained using the authors' software, transforming the GAB sigmoid into a second degree parabola and fitting it using least squares.

For the results of EMC, chemical composition, ultrastructural organisation and –OH group concentration, ANOVA was performed with a confidence level of 95%, followed by LSD analysis. Before ANOVA was performed, normality, independence and homoscedasticity of the data were determined using skewness and kurtosis values and the Levene test.

3 Results and discussion

In all cases, EMC values were lower in the thermally modified wood than in the untreated wood, and therefore the three isotherms of the modified wood were below those of the untreated wood (Table S1, Fig. S1, see Supplementary material), agreeing with the results of previous studies (Hill et al. 2012; Olek et al. 2012; Rautkari et al. 2013; Kymäläinen et al. 2015, 2018; Sun et al. 2017; Hosseinpourpia et al. 2017, 2018; Li et al. 2017; Wang et al. 2018; Tarmian and Mastouri 2019). All the isotherms were type II sigmoid ($C_g > 2$) and their fits using the GAB model were considered valid in all cases because the RMSE was less than 4% and R was greater than 0.990 (Avramidis 1997) (Table 1).

Although the physical interpretation of isotherms parameters using the traditional models (GAB, Dent, HH) is still in dispute (Zelinka et al. 2018), in this study they were interpreted in the usual manner, given that this matter still needs considerable investigation. The X_m content contributed by the monolayer was in all cases lower in the thermally modified wood than in the untreated wood, for all isotherms. Moreover, the point of inflexion from which the multilayer prevails over the monolayer is at around 30% (32.7–34.0) in the untreated wood and around 40% (38.2–41.2) in the thermally modified wood. This means that the multilayer contribution to EMC in the thermally modified wood was lower than in the untreated wood (Table 1). These values are similar to those obtained in other studies in which wood degraded naturally (Esteban et al. 2009, 2010; Simón et al. 2017) but no significant differences were observed between the points of inflexion, as in this case.

The isotherms of the thermally modified wood are more linear; i.e., they are less sigmoid in shape than in the untreated wood. Moreover, in agreement with Hill (2006), the hysteresis loop area is smaller in the thermally modified wood than in the untreated wood. This means that the wood is more stable, because it has less free energy in the sorption process (Siau 1995; Esteban et al. 2005, 2008a, b) (Fig. 1). The same was found after analysing the derivatives of the isotherms. In all cases the slope of the thermally modified wood curve is lower than for the untreated wood, and thus for any given RH interval, the difference in EMC is lower (Fig. S2, see Supplementary material). However, most studies of thermally modified wood (Hill 2006; Hill et al. 2009, 2012; Kymäläinen et al. 2015, 2018; Sun et al. 2017; Hosseinpourpia et al. 2017, 2018) reported a downward trend in the hysteresis loop as the temperature increases to glass temperature, following the hysteresis model of glassy solids (Hill et al. 2009, 2010). Other studies (Militz 2002) reported that heat treatment had no influence on the hysteresis loop, or even displayed an opposite trend (Olek et al. 2012), with the area of the loop increasing in poplar and beech wood. These differences may be due to several factors such as the methodology and parameters of the process, given that mild heat treatment increases hysteresis, but as the intensity of the treatment increases, hysteresis decreases (Jalaludin et al. 2010). The decrease in the hysteresis area in this study can be attributed to the combined action of the lower number of active sites and the change in the porosity of the cell wall nanopores (Kymäläinen et al. 2015). Although this study revealed significant differences between the number of active sites in untreated and thermally modified wood (Table 2), Rautkari et al. (2013) reported that the decrease in hygroscopicity cannot be explained solely by the availability of active sites, because there is a poor correlation between EMC and the amount of accessible hydroxyl groups determined by the deuterium exchange method. These authors posited that there must be an additional mechanism to control EMC other than the available

Table 1 GAB fitting parameters for 15 °C, 35 ºC and 50 °C isotherms of untreated and thermally modified wood

	15 ºC isotherm		35 ºC isotherm		50 ºC isotherm	
	Untreated wood	Thermally modified wood	Untreated wood	Thermally modified wood	Untreated wood	Thermally modified wood
Adsorption						
X_m	$8.08^A \pm 0.23$	$7.02^B \pm 0.18$	$6.84^A \pm 0.10$	$6.77^A \pm 0.17$	$6.74^A \pm 0.11$	$6.40^B \pm 0.20$
K	0.74 ± 0.26	0.63 ± 0.21	0.76 ± 0.13	0.62 ± 0.20	0.75 ± 0.12	0.62 ± 0.24
C_g	8.05 ± 0.04	8.45 ± 0.03	7.23 ± 0.02	8.12 ± 0.04	6.60 ± 0.03	7.88 ± 0.04
R	0.994	0.997	0.998	0.996	0.998	0.996
RMSE (%)	1.35	0.56	0.27	0.55	0.26	0.45
RH (%)	33.90	39.80	32.70	40.20	32.90	40.30
EMC_a (%)	7.84	6.91	6.42	6.59	6.12	6.17
EMC_f (%)	0.24	0.12	0.42	0.18	0.62	0.23
Desorption						
X_m	$8.85^A \pm 0.23$	$8.12^B \pm 0.13$	$8.22^A \pm 0.11$	$7.54^B \pm 0.17$	$7.92^A \pm 0.15$	$7.31^B \pm 0.14$
K	0.76 ± 0.26	0.65 ± 0.15	0.73 ± 0.11	0.62 ± 0.20	0.72 ± 0.14	0.61 ± 0.24
C_g	8.48 ± 0.04	8.40 ± 0.02	7.01 ± 0.02	8.70 ± 0.03	5.98 ± 0.03	7.79 ± 0.03
R	0.992	0.996	0.998	0.996	0.997	0.997
RMSE (%)	1.34	0.29	0.28	0.58	0.52	0.23
RH (%)	32.90	38.70	34.00	40.50	33.8	41.60
EMC_d (%)	8.72	7.98	7.63	7.48	6.88	7.02
EMC_f (%)	0.13	0.14	0.59	0.06	1.04	0.29

X_m: Monolayer saturation moisture content (%); K: constant; C_g: Guggenheim constant; R: correlation coefficient; RMSE: Root Medium Square Error; RH: relative humidity; EMCa: moisture content contributed by the monolayer in adsorption before the point of inflexion; EMCd: moisture content contributed by the monolayer in desorption before the point of inflexion; EMCf: water taken up via monolayer sorption after the point of inflexion. Different superscript indicates significant differences

Fig. 1 Area of the hysteresis loop in untreated and thermally modified wood for the 15°, 35° and 50 °C isotherms
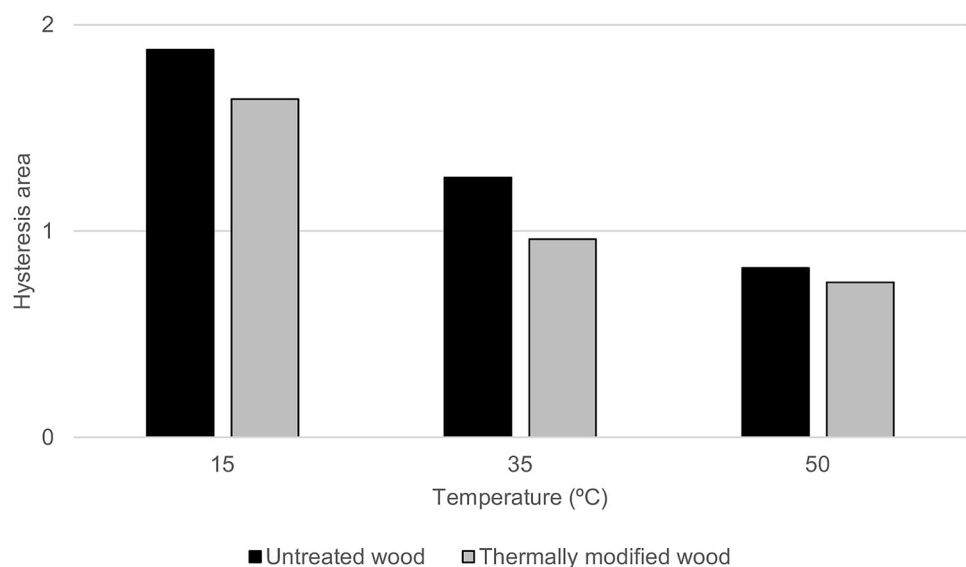
hydroxyl groups, as suggested by Hill et al. (2012), in which thermally modified wood, by causing heat degradation of the hemicellulose and possibly of the amorphous cellulose, together with an increase in lignin reticulation, would increase the stiffness of the cell wall matrix. This increased stiffness limits expansion of the cell wall nanopores even further, leading to a decrease in EMC (Keating et al. 2013; Popescu and Hill 2013).

The changes in the chemical composition of the cell wall components after heat treatment could also explain

Table 2 Theoretical number of –OH groups and number of accessible –OH groups

	Number of theoretical –OH groups (mmol g^{-1})	σ	Estimated number of accessible –OH groups (Crystallinity index of cellulose considered) (mmol g^{-1})	σ
Untreated wood	13.29[a]	0.06	10.25[a]	0.05
Thermally modified wood	13.91[b]	0.05	9.95[b]	0.03

Different letters indicate statistically significant differences

the decrease in EMC. Heat treatment increases cellulose, lignin and extractives contents and decreases hemicellulose content (Table S2, see Supplementary material) (Fig. 2). These results agree with those of other studies (Rautkari et al. 2013; Sun et al. 2017; Li et al. 2017; Kymäläinen et al. 2018; Wang et al. 2018), and it is precisely the hemicellulose degradation caused by the high temperature of 160–260 °C (Rowell et al. 2009; Kasemsiri et al. 2012; Mahnert et al. 2013; Xing and Li 2014) that contributes most to the decrease in EMC, because hemicelluloses contribute the highest amount of -OH groups to the cell wall, followed by cellulose and lignin (Christensen and Kelsey 1959).

With regard to cellulose, the conversion of amorphous regions into more thermally stable crystalline regions (Fengel and Wegener 1989) may also have contributed to a lower amount of accessible –OH groups and therefore lower EMC.

The relative lignin content also increased, concurring with the results of Kamdem et al. (2002) and Boonstra and Tjeerdsma (2006), and although it is accepted that lignin is the most thermally stable component of the cell wall (Hill 2006), some thermal degradation of lignin at relatively low temperatures can occur, producing various phenolic decomposition products (Sandermann and Augustin 1964) and emergence of new cross-links in the lignin network structure (Hill 2006). However, it remains unclear how this contributes to wood hygroscopicity.

In addition, as in other studies (Biziks et al. 2014; Čermák et al. 2015), an increase occurred in the relative extractives content in the thermally modified wood. This phenomenon could fill the nanopores in the cell wall matrix, especially in hardwoods, in which the extractive percentages are higher and can be multiplied ×10 depending on the type of thermal treatment, thus decreasing the penetration of water molecules and causing a decrease in wood hygroscopicity, manifested in the decrease in EMC after thermal modification (Biziks et al. 2014; Wentzel et al. 2018). However, the low extractives content in the thermally treated wood in this work would probably not have affected the EMC content.

Contrary to expectations, the FTIR spectra (Table S3 see Supplementary material) (Fig. 3), show the same peaks, and no significant changes were detected. Due to the degradation of the cellulose, the carbonyl peak should have been affected, but this did not happen. The statistically significant difference of the hemicellulose content (Table S2, see Supplementary material), 28.04% in untreated wood compared to 22.08% in treated wood, was not sufficient to cause the disappearance of the carbonyl group. This decrease in the hemicellulose content definitely contributed to the decrease in EMC, although other, unknown, changes produced inside the ultrastructure need to be identified to explain the influence of the thermal treatments on the cell wall.

2D XRD of the wood samples shows a characteristic fibre texture pattern with intensities concentrated in

Fig. 2 Contents of the main components of untreated and thermally modified wood
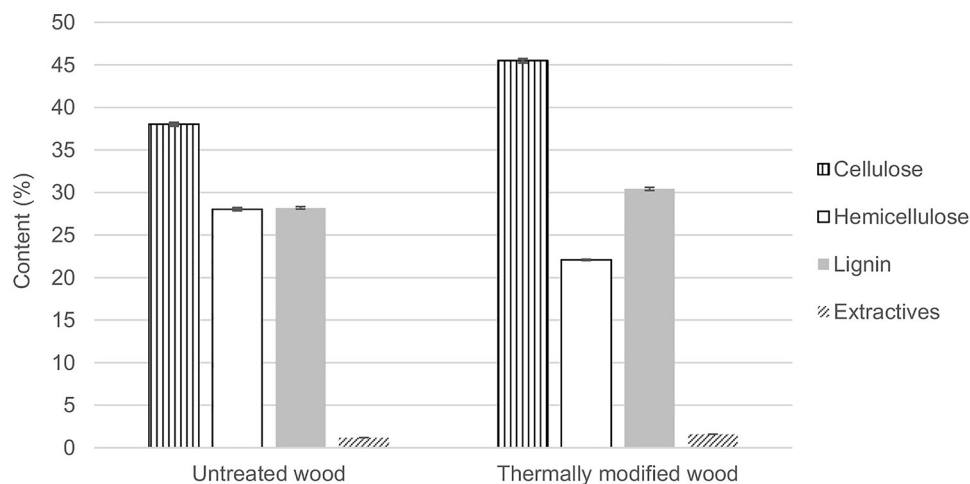
Fig. 3 IR spectrogram of untreated and thermally modified wood
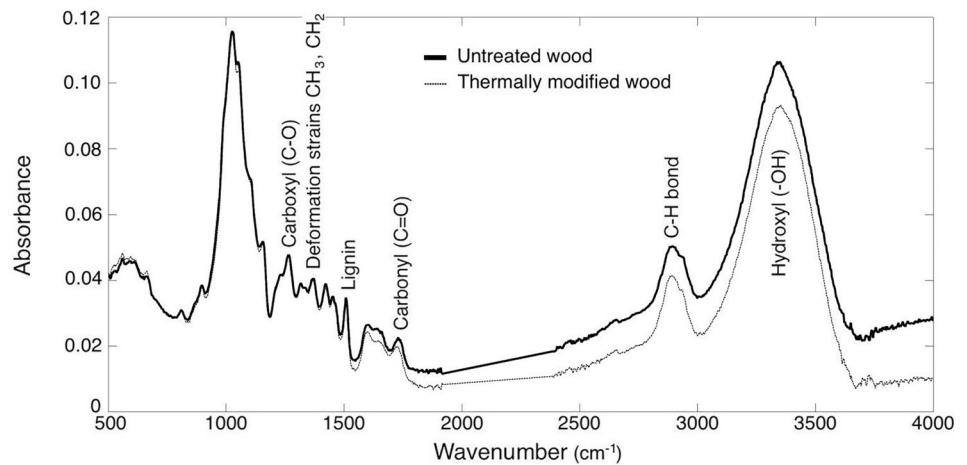
**Table 3** Cellulose crystallite size and orientation parameters of untreated and thermally modified wood samples

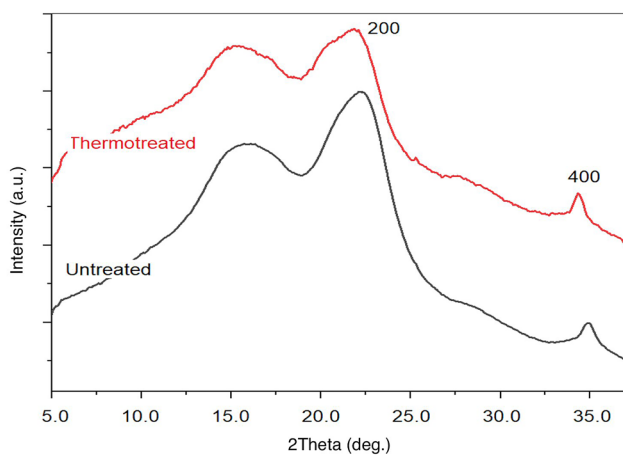| Crystallite size (Å)		Untreated	Thermally modified
Whole	c-axis	95.1 ± 7.4	131.0 ± 15.0
Whole	a-axis	23.8 ± 2.0	26.9 ± 3.9
Oriented	c-axis	116.7 ± 8.2	122.9 ± 12.0
Oriented	a-axis	27.2 ± 0.4	30.2 ± 0.1
Random	c-axis	48.4 ± 2.9	44.2 ± 4.6
Random	a-axis	23.4 ± 2.0	23.9 ± 5.1
AS_200 (°)		51.8 ± 0.7	31.1 ± 11.7
Oriented fraction		0.39 ± 0.03	0.69 ± 0.44

AS_200 is the angular spread of arcs displayed in the 200 reflection

arcs due to the preferred orientation of cellulose crystals with their c-axis aligned parallel to the fibres and rotated around the fibre axis (Table 3, Fig. 4). This effect is more obvious for 004 and 200 cellulose reflections, which are related to orthogonally oriented crystal directions (c- and a-axis, respectively). The angular spread (AS_200) of arcs

displayed in the 200 reflection rings (Debye rings) can be used to measure scattering in cellulose crystal orientation. The value for AS_200, calculated from gamma scans for the 200 cellulose main reflection, ranges from 51.8° for untreated wood (*P. radiata* untreated) to 31.1° in thermally modified wood (*P. radiata* thermally modified) (Table 3). The 2D XRD patterns allow differentiation between the randomly oriented cellulose fraction, which contributes homogeneously to the whole Debye ring, and the highly crystalline cellulose fraction, which shows a strong preferential orientation and contributes to the arcs. The contribution of this poorly crystalline randomly oriented region decreases with heat treatment (higher oriented fraction values). Additionally, 2Theta-scans of the wood samples calculated from 2D XRD patterns show highly anisotropic peak broadening as cellulose crystals are elongated along the c-axis, producing sharper peaks for the 004 reflections (0.5°–1.0°) than for the 200 reflections (2.8°–3.7°) (Fig. 5). Crystallite size along the c-axis and a-axis, calculated from the peak broadening of 004 and 200 reflections using the Scherrer equation, is about 120 and 25 Å, respectively. XRD data also shows that the

Fig. 4 2D XRD pattern of *P. radiata* wood samples analysed with their fibres oriented perpendicular to the X-ray beam. **a** Untreated; **b** Thermally modified
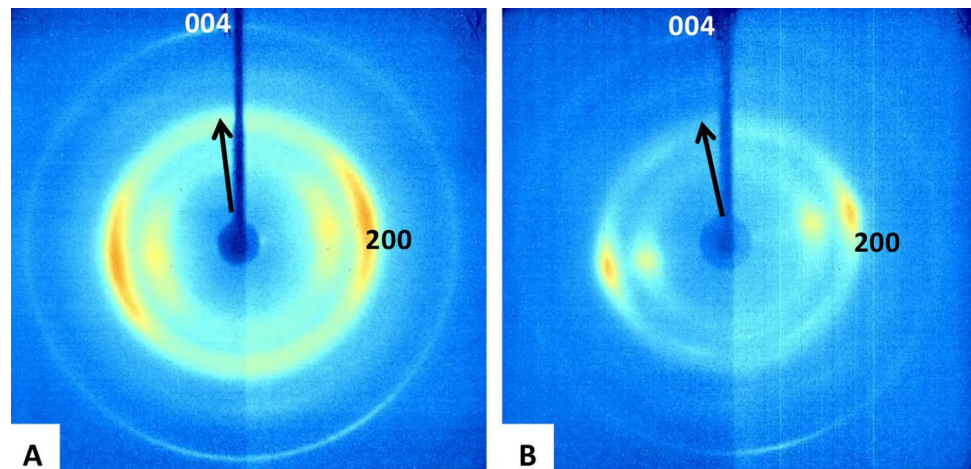
Fig. 5 Calculated 2Theta scan from 2D XRD patterns of untreated and thermally modified *P. radiata* samples

Table 4 Crystallinity data from Rietveld refinement analysis of X-ray powder diffraction patterns

	CrI (%)		D_{200} (Å)	
	$\bar{x}$	σ	$\bar{x}$	σ
Untreated wood	43.20[a]	1.99	20.97[a]	0.15
Thermally modified wood	47.00[a]	4.42	24.70[b]	0.78

CrI(%) Crystallinity index; D_{200} Mean crystal size

thermally modified *P. radiata* wood has greater crystallinity (larger crystallite sizes), particularly for the preferentially oriented (Oriented) cellulose fraction (Table 3). During heating, the average crystallite size (Whole) for cellulose became closer to that of the oriented highly crystalline cellulose regions (Oriented), demonstrating that most of the less ordered poorly crystalline regions of cellulose (Random) reorganise and recrystallise, acquiring a configuration closer to the oriented highly crystalline cellulose regions.

Other authors obtained similar results (Table 4), reporting that wood crystallinity increases after heat treatment (Bhuiyan et al. 2000; Akgul et al. 2007; Huang et al. 2012; Yildiz and Gümüskaya 2007; Wang et al. 2018). The higher crystallinity means that there is a reduction of polar sites available. The increase in crystallinity can be explained by the decomposition of amorphous regions in the cellulose (Boonstra and Tjeersma 2006; Wikberg and Maunu 2004; Bhuiyan and Hirai 2005) and hemicellulose (Hill 2006; Olek and Bonarski 2014) or by crystallisation of amorphous cellulose (Esteves and Pereira 2009; Inagaki et al. 2010; Olek and Bonarski 2014). Other authors explained the increase in crystallinity by the increased mobility of cellulose chains in conditions of high humidity and high temperatures (Bhuiyan et al. 2000), causing a reorganisation or reorientation of the paracrystalline regions (Bhuiyan et al. 2000; Olek and

Bonarski 2014; Xing et al. 2016; Yin et al. 2017) of the cellulose molecules, where crystallite size can also increase. This ultrastructural reorganisation of cellulose from paracrystalline (less ordered) to crystalline state causes a further decrease in the available sorption sites (Jalaludin et al. 2010). Hill (2006) confirmed that during thermal modification, part of the paracrystalline cellulose with accessible –OH groups became crystalline with blocked –OH groups. These two mechanisms, recrystallisation of paracrystalline regions and orientation of crystalline regions, could explain the thermally induced structural changes observed in *P. radiata* wood in this study. This orientation process could be due to a propagation of the crystallisation front of cellulose by epitaxy (oriented nucleation and growth) starting from the oriented highly crystalline regions during the recrystallisation process. This would explain the increase in the degree of crystal orientation (lower values of AS_200), higher Oriented fraction values and larger crystallite size values. Thus, in thermally treated wood, most of the cellulose is in highly crystalline, highly ordered regions.

2D XRD shows that the thermally induced recrystallisation of cellulose responsible for increasing wood crystallinity also causes an ultrastructural reorganisation, with greater cellulose crystal orientation. Changes in crystallographic orientation (texture) in thermally treated wood have been reported by other authors, showing a complex response depending on the temperature range (Olek and Bonarski, 2014).

4 Conclusion

Heat treatment caused changes in the hygroscopicity and chemical composition of the wood and a reorganisation of the cellulose. The thermally modified wood is less hygroscopic than the untreated wood because the EMC is lower. The hysteresis loop areas are smaller and the slopes of the derivatives of the isotherms are lower, indicating that the thermally modified wood is more hygroscopically stable. In addition, the points of inflexion are higher in the multilayer, indicating a lower contribution of the multilayer to EMC in the thermally modified wood. The thermal modification also caused chemical changes in the cell wall components, comprising hemicellulose degradation and an increase in the relative proportion of the other main components (cellulose, lignin and extractives). However, despite the chemical changes caused by the thermal modification, the characteristic peaks of the infrared spectra experienced no substantial changes. Lastly, the crystallinity and the degree of cellulose crystal orientation increased. Less ordered poorly crystalline regions of cellulose reorganise and recrystallise, acquiring the configuration of oriented highly crystalline cellulose regions. This reorganisation could be explained by epitaxial

growth of cellulose starting from the highly oriented crystalline regions during the recrystallisation process.

References

Acheson DT (1965) Vapor pressure of saturated aqueous salt solutions, humidity and moisture, vol 3. Rein hold Publishing Corporation, New York

Akgul M, Gumuskaya E, Korkut S (2007) Crystalline structure of heat-treated Scots pine (*Pinus sylvestris* L.) and Uludag fir (*Abies nordmanniana* (Stev.) subsp. *bornmuelleriana* (Mattf.)) wood. Wood Sci Technol 41:281–289. https://doi.org/10.1007/s00226-006-0110-9

Avramidis S (1997) The basics of sorption. In: Paper presented at the proceedings of international conference of COST Action E8: mechanical performance of wood and wood products. Copenhagen, pp 1–16

Baxter GP, Cooper WC Jr (1924) The aqueous pressure of hydrated crystal s. II. Oxalic acid, sodium sulfate, sodium acetate, sodium carbonate, di sodium phosphate, barium chloride. J Am Chern Soc 46:923

Bhuiyan T, Hirai N (2005) Study of crystalline behavior of heat-treated wood cellulose during treatments in water. J Wood Sci 51:42–47

Bhuiyan MTR, Hirai N, Sobue N (2000) Changes of crystallinity in wood cellulose by heat treatment under dried and moist conditions. J Wood Sci 46(6):431–436. https://doi.org/10.1007/BF00765800

Biziks V, Andersons B, Sansonetti E, Andersone I, Militz H, Grinins J (2014) One-stage thermo-hydro treatment (THT) of hardwoods: an analysis of form stability after five soaking-drying cycles. Holzforschung 69(5):563–571

Bonarski JT, Olek W (2011) Application of the crystalline volume fraction for characterizing the ultrastructural organization of wood. Cellulose 18:223–235

Boonstra MJ, Tjeerdsma B (2006) Chemical analysis of heat treated softwoods. Holz Roh Werkst 64(3):204–211

Boonstra MJ, van Acker J, Kegel E, Stevens M (2007) Optimisation of a two-stage heat treatment process: durability aspects. Wood Sci Technol 41:31–57. https://doi.org/10.1007/s00226-006-0087-4

Čermák P, Rautkari L, Horacek P, Saake B, Rademacher P, Sablık P (2015) Analysis of dimensional stability of thermally modified wood affected by re-wetting cycles. BioResources 10(2):3242–3253

Christensen GN, Kelsey KE (1959) The rate of sorption of water vapor by wood. Holz Roh Werkst 17:178–188

Clarke ECW, Glew DN (1985) Evaluation of the thermodynamic functions for aqueous sodium chloride from equilibrium and calorimetric measurements below 154 °C. J Phys Chem Ref Data 14:489–610

Easty DB, Malcolm EW (1982) Estimation of pulping yield in continuous digesters from carbohydrate and lignin determinations. Tappi J 65:78–80

Esteban LG, Gril J, Palacios P, Guindeo A (2005) Reduction of wood hygroscopicity and associated dimensional response by repeated humidity cycles. Ann For Sci 62:275–284

Esteban LG, de Palacios P, Fernandez FG, Guindeo A, Cano NN (2008a) Sorption and thermodynamic properties of old and new *Pinus sylvestris* wood. Wood Fiber Sci 40:111–121

Esteban LG, de Palacios P, Fernandez FG, Guindeo A, Conde M, Baonza V (2008b) Sorption and thermodynamic properties

of juvenile *Pinus sylvestris* L. wood after 103 years of submersion. Holzforschung 62:745–751. https://doi.org/10.1515/HF.2008.106

Esteban LG, de Palacios P, García Fernandez F, Martin JA, Genova M, Fernandez-Golfin JI (2009) Sorption and thermodynamic properties of buried juvenile *Pinus sylvestris* L. wood aged 1,170 ± 40 BP. Wood Sci Technol 43:140–151. https://doi.org/10.1007/s00226-009-0261-6

Esteban LG, de Palacios P, García Fernandez F, García-Amorena I (2010) Effects of burial of *Quercus* spp. wood aged 5910±250 BP on sorption and thermodynamic properties. Int Biodeter Biodegrad 64:371–377. https://doi.org/10.1016/j.ibiod.2010.01.010

Esteves BM, Pereira HM (2009) Wood modification by heat treatment: a review. BioResources 4(1):370–404

Evans R, Newman RH, Roick UC (1995) Changes in cellulose crystallinity during kraft pulping. Comparison of infrared, x-ray diffraction and solid state NMR results. Holzforschung 49:498–504

Fengel D, Wegener G (1989) Wood: chemistry ultrastructure. Reactions. Walter De Gruyter, Berlin

Fredriksson M, Thybring EE (2018) Scanning or desorption isotherms? Characterising sorption hysteresis of wood. Cellulose 25(8):4477–4485. https://doi.org/10.1007/s10570-018-1898-9

French AD, Kim HJ (2018) Cotton fiber structure. In: Fang D (ed) Cotton fiber: physics and biology. Springer, New York, pp 13–39

French AD, Santiago Cintrón M (2013) Cellulose polymorphy, crystallite size and the Segal Crystallinity Index. Cellulose 20:583–588. https://doi.org/10.1007/s10570-012-9833-y

García-Iruela A, Esteban LG, de Palacios P, García Fernández F, Martín-Sampedro R, Eugenio ME (2019) Changes in cell wall components of *Pinus sylvestris* L. wood after 300 years in contact with salt (NaCl). BioResources 14(2):3069–3091

Greenspan L (1977) Humidity fixed-points of binary saturated aqueous solutions. J Res Nat Bureau Stand Sect A Phys Chem 81(1):89–96

Hakkou M, Pétrissans M, Gérardin P, Zoulalian A (2006) Investigations of the reasons for fungal durability of heat-treated beech wood. Polym Degrad Stab 91:393–397

He J, Cui S, Wang SY (2008) Preparation and crystalline analysis of high-grade bamboo dissolving pulp for cellulose acetate. J Appl Polym Sci 107:1029–1038

Hill CAS (2006) Wood modification—chemical thermal and other processes. Wiley, Chichester

Hill CAS, Jones D (1996) The dimensional stabilisation of Corsican pine sapwood by reaction with carboxylic acid anhydrides. The effect of chain length. Holzforschung 50:457–462. https://doi.org/10.1515/hfsg.1996.50.5.457

Hill CAS, Jones D (1999) Dimensional changes in Corsican pine sapwood due to chemical modification with linear chain anhydrides. Holzforschung 53:267–271. https://doi.org/10.1515/HF.1999.045

Hill CAS, Norton A, Newman G (2009) The water vapor sorption behavior of natural fibers. J Appl Polym Sci 112:1524–1537

Hill C, Norton AJ, Newman G (2010) The water vapour sorption properties of Sitka spruce determined using a dynamic vapour sorption apparatus. Wood Sci Technol 44:497–514. https://doi.org/10.1007/s00226-010-0305-y

Hill C, Ramsay J, Keating B, Laine K, Rautkari L, Hughes M, Constant B (2012) The water vapour sorption properties of thermally modified and densified wood. J Mater Sci 47(7):3191–3197. https://doi.org/10.1007/s10853-011-6154-8

Hosseinpourpia R, Adamopoulos S, Holstein N, Mai C (2017) Dynamic vapour sorption and water-related properties of thermally modified Scots pine (*Pinus sylvestris* L.) wood pre-treated with proton acid. Polym Degrad Stabil 138:161–168

Hosseinpourpia R, Adamopoulos S, Mai C (2018) Effects of acid pre-treatments on the swelling and vapor sorption of thermally modified scots pine (*Pinussylvestris* L.) wood. BioResources 13(1):331–345

Huang PH (1985) Electrical and thermodynamic characterization of water-vapor polymeric film system for humidity sensing. Sens Actuators 8(1):23–28

Huang X, Kocaefe D, Kocaefe Y, Boluk Y, Pichette A (2012) Study of the degradation behavior of heat-treated jack pine (*Pinus banksiana*) under artificial sunlight irradiation. Polym Degrad Stabil 97(7):1197–1214. https://doi.org/10.1016/j.polymdegradstab.2012.03.022

Inagaki T, Siesler HW, Mitsui K, Tsuchikawa S (2010) Difference of the crystal structure of cellulose in wood after hydrothermal and aging degradation: a NIR spectroscopy and XRD study. Biomacromol 11(9):2300–2305. https://doi.org/10.1021/bm100403y

Jalaludin Z, Hill CAS, Xie Y, Samsi HW, Husain H, Awang K, Curling SF (2010) Analysis of the water vapour sorption isotherms of thermally modified acacia and sesendok. Wood Materi Sci Eng 5(3–4):194–203

Jones PD, Schimleck LR, Peter GF, Daniels RF, Clark A III (2006) Nondestructive estimation of wood chemical composition of sections of radial wood strips by diffuse reflectance near infrared spectroscopy. Wood Sci Technol 40:709–720. https://doi.org/10.1007/s00226-006-0085-6

Jowitt R, Wagstaffe PJ (1989) The certification of water content of microcrystalline cellulose (MCC) at 10 water activities. Commission of the European Communities. Community Bureau of Reference. BCR, CRM, EUR 12429, EN, Brussels, Belgium 302

Kamdem DP, Pizzi A, Jermannaud A (2002) Durability of heat-treated wood. Holz Roh Werkst 60(1):1–6

Kasemsiri P, Hiziroglu S, Rimdusit S (2012) Characterization of heat treated Eastern red cedar (*Juniperusvirginiana* L.). J Mater Process Techol 212:1324–1330. https://doi.org/10.1016/j.matprotec.2011.12.019

Keating BA, Hill CAS, Sun D, English R (2013) The water vapour sorption behaviour of a galactomannan cellulose nanocomposite film analysed using parallel exponential kinetics and the Kelvin-Voigt viscoelastic model. J Appl Polym Sci 129(4):2352–2359

Kim G, Yun K, Kim J (1998) Effect of heat treatment on the decay resistance and the bending properties of radiata pine sapwood. Mater Organismen 32(2):101–108

Kim HJ, Liu Y, French AD, Lee CM, Kim SH (2018) Comparison and validation of Fourier transform infrared spectroscopic methods for monitoring secondary cell wall cellulose from cotton fibers. Cellulose 25:49–64. https://doi.org/10.1007/s10570-017-1547-8

Kymäläinen M, Rautkari L, Hill CAS (2015) Sorption behaviour of torrefied wood and charcoal determined by dynamic vapour sorption. J Mater Sci 50:7673–7680. https://doi.org/10.1007/s10853-015-9332-2

Kymäläinen M, Ben Mlouka S, Belt T, Merk V, Liljeström V, Hänninen T, Uimonen T, Kostiainen M, Rautkari L (2018) Chemical, water vapour sorption and ultrastructural analysis of Scots pine wood thermally modified in high-pressure reactor under saturated steam. J Mater Sci 53(4):3027–3037. https://doi.org/10.1007/s10853-017-1714-1

Li T, Cheng D, Avramidis S, Walinder MEP, Zhou D (2017) Response of hygroscopicity to heat treatment and its relation to durability of thermally modified wood. Constr Build Mater 144:671–676

Ling Z, Wang T, Makarem M, Santiago-Cintrón M, Cheng HN, Kang X, Bacher M, Potthast A, Rosenau T, King H, Delhom CD, Nam S, Edwards JV, Kim SH, Xu F, French AD (2019) Effects of ball milling on the structure of cotton cellulose. Cellulose 26:305–328. https://doi.org/10.1007/s10570-018-02230-x

Mahnert KC, Adamopoulos S, Koch G, Militz H (2013) Topochemistry of heat-treated and N-methylol melamine-modified wood of koto (*Pterygotamacrocarpa* K. Schum) and limba (*Terminalia superba* Engl. & Diels). Holzforschung 67(2):137–146. https://doi.org/10.1515/hf-2012-0017

Militz H (2002) Heat treatment of wood: European processes and their background. In: Paper presented at the proceedings of conference on enhancing the durability of lumber and engineered wood products, 11–13 Feb 2002 Kissimmee, Orlando

Nishiyama Y, Langan P, Chanzy H (2002) Crystal structure and hydrogen-bonding system in cellulose Ib from synchrotron X-ray and neutron fiber diffraction. J Am Chem Soc 124:9074–9082

Olek W, Bonarski JT (2014) Effects of thermal modification on wood ultrastructure analyzed with crystallographic texture. Holzforschung 68:721–726. https://doi.org/10.1515/hf-2013-0165

Olek W, Majka J, Czajkowski Ł (2012) Sorption isotherms of thermally modified wood. Holzforschung 67:183–191

Park S, Johnson DK, Ishizawa CI, Parilla PA, Davis MF (2009) Measuring the crystallinity index of cellulose by solid state 13C nuclear magnetic resonance. Cellulose 16(4):641–647. https://doi.org/10.1007/s10570-009-9321-1

Park S, Baker JO, Himmel ME, Parilla PA, Johnson DK (2010) Cellulose crystallinity index: measurement techniques and their impact on interpreting cellulase performance. Biotechnol Biofuels 3:10. https://doi.org/10.1186/1754-6834-3-10

Popescu CM, Hill CAS (2013) The water vapour adsorption-desorption behavior of naturally aged *Tiliacordata* Mill. wood. Polym Degrad Stabil 98(9):1804–1813

Rautkari L, Hill CS, Curling S, Jalaludin Z, Ormondroyd G (2013) What is the role of the accessibility of wood hydroxyl groups in controlling moisture content? J Mater Sci 48:6352–6356. https://doi.org/10.1007/s10853-013-7434-2

Rautkari L, Honkanen J, Hill CAS, Ridley-Ellis D, Hughes M (2014) Mechanical and physical properties of thermally modified Scots pine wood in high pressure reactor under saturated steam at 120, 150 and 180 C. Eur J Wood Prod 72(1):33–41. https://doi.org/10.1007/s00107-013-0749-5

Rietveld H (1969) A profile refinement method for nuclear and magnetic structures. J Appl Crystallogr 2:65–71

Rowell RM (1980) Distribution of reacted chemicals in southern pine modified with methyl isocyanate. Wood Sci 13:102–110

Rowell RM, Ibach ER, McSweeny J, Nilsson T (2009) Understanding decay resistance dimensional stability and strength changes in heat treated and acetylated wood. In: Proceedings of the 4th European conference on wood modification, Stockholm, Sweden, pp 489–502. https://doi.org/10.1080/17480270903261339

Sandermann W, Augustin H (1964) Chemical investigations on the thermal decomposition of wood—Part III: chemical investigation on the course of decomposition. Holz Roh Werkst 22(10):377–386

Segal L, Creely JJ, Martin AE, Conrad CM (1959) An empirical method for estimating the degree of crystallinity of native cellulose using the X-ray diffractometer. Text Res J 29:786–794. https://doi.org/10.1177/004051755902901003

Siau JF (1995) Wood: influence of moisture on physical properties. Department of Wood Science and Forest Products, Virginia Polytechnic Institute and State University, Blacksburg

Simón C, Esteban LG, de Palacios P, Fernandez FG, García-Iruela A, Martín-Sampedro R, Eugenio ME (2017) Sorption and thermodynamic properties of wood of *Pinus canariensis* C. Sm. ex DC. buried in volcanic ash during eruption. Wood Sci Technol 51:517–534. https://doi.org/10.1007/s00226-016-0884-3

Sluiter A, Ruiz R, Scarlata C, Sluiter J, Templeton D (2005) Determination of extractives in biomass. National Renewable Energy Laboratory (NREL) Laboratory Analytical Procedure (LAP). http://www.nrel.gov/biomass/pdfs/42619.pdf. Accessed 27 Mar 2015

Sluiter A, Hames B, Ruiz R, Scarlata C, Sluiter J, Templeton D, Crocker S (2012) Determination of structural carbohydrates and lignin in biomass. National Renewable Energy Laboratory (NREL) Laboratory Analytical Procedure (LAP). http://www.nrel.gov/biomass/pdfs/42618.pdf. Accessed 27 Mar 2015

Sun B, Wang Z, Liu JJ (2017) Changes of chemical properties and the water vapour sorption of *Eucalyptus pellita* wood thermally modified in vacuum. Wood Sci 63(2):133–139. https://doi.org/10.1007/s10086-016-1601-4

Tarmian A, Mastouri A (2019) Changes in moisture exclusion efficiency and crystallinity of thermally modified wood with aging. IForest 12(1):92–97. https://doi.org/10.3832/ifor2723-011

ThermoWood® Handbook (2003) Finnish Thermowood Association

Thybring EE, Thygesen LG, Burgert I (2017) Hydroxyl accessibility in wood cell walls as affected by drying and re-wetting procedures. Cellulose 24:2375–2384. https://doi.org/10.1007/s10570-017-1278-x

Thygesen A, Oddershede J, Lilholt H, Thomsen AB, Stahl K (2005) On the determination of crystallinity and cellulose content in plant fibres. Cellulose 12:563–576

Wang X, Chen X, Xie X, Wu Y, Zhao L, Li Y, Wang S (2018) Effects of thermal modification on the physical, chemical and micromechanical properties of Masson pine wood (*Pinusmassoniana* Lamb.). Holzforschung 72(12):1063–1070. https://doi.org/10.1515/hf-2017-0205

Wentzel M, Altgen M, Militz H (2018) Analyzing reversible changes in hygroscopicity of thermally modified eucalypt wood from open and closed reactor systems. Wood Sci Technol 52(4):889–907. https://doi.org/10.1007/s00226-018-1012-3

Wikberg H, Maunu S (2004) Characterisation of thermally modified hard- and softwoods by 13C CPMAS NMR. Carbohydr Polym 58:461–466

Xing D, Li J (2014) Effects of heat treatment on thermal decomposition and combustion performance of *Larix* spp. Wood Bioresour 9(3):4274–4287

Xing D, Li J, Wang X, Wang S (2016) In situ measurement of heat-treated wood cell wall at elevated temperature by nanoindentation. Ind Crops Prod 87:142–149

Yildiz S, Gümüskaya E (2007) The effects of thermal modification on crystalline structure of cellulose in soft and hardwood. Build Environ 42:62–67

Yin J, Yuan T, Lu Y, Song K, Li H, Zhao G, Yin Y (2017) Effect of compression combined with steam treatment on the porosity, chemical composition and cellulose crystalline structure of wood cell walls. Carbohydr Polym 155:163–172

Young RA (ed) (1993) The Rietveld method. IUCr monographs in crystallography, 5. International Union of Crystallography. Oxford University Press, New York, p 298

Zelinka SL, Glass SV, Thybring EE (2018) Myth versus reality: do parabolic sorption isotherm models reflect actual wood–water thermodynamics? Wood Sci Technol 52:1701–1706. https://doi.org/10.1007/s00226-018-1035-9